Cortical rigidity of round cells in mitotic phase and suspended state

Yuji Shimizu[†], Seyed Mohammad Ali Haghparast[†], Takanori Kihara[*], Jun Miyake

Department of Mechanical Science and Bioengineering, Graduate School of Engineering Science, Osaka University, 1-3 Machikaneyama, Toyonaka, Osaka 560-8531, Japan

[†]These authors contributed equally.

[*]Corresponding author. Tel: +81-6-6850-6550, Fax: +81-6-6850-6557

E-mail address: takanori.kihara@gmail.com (T. Kihara)

Abstract

This paper describes the results of the analysis of cortical rigidity in two round cell states: mitotic round cells and detached round cells after trypsinization using atomic force microscopy (AFM). These two states are primary cell events with dynamic morphological alterations in vitro. The trypsinized detached cells were fixed on the substrate of membrane anchoring oleyl surface. Fluorescent images taken by confocal laser scanning microscopy revealed diverse cell surface protrusions and cortical actin development in the round cells under different conditions. Although the cortical actin of these cells seemed to develop similarly, cortical rigidity of the trypsinized round cells showed greater stiffness than that of mitotic round cells. The elasticity measurements by AFM may detect invisible information about the maturation or strength of F-actin structures and such measurements may indicate that the strength of the actomyosin cortex would be higher in trypsinized round cells compared to mitotic cells. The mechanical properties can help provide better insights into the characteristics of the actin cytoskeletlon network in vicinity of cell surface during dynamic morphological alterations.

Keywords: Mechanical property; Cortical actin; Mitotic phase; Trypsinized round cell; Atomic force microscopy; Surface protrusions

Abbreviations: AFM, atomic force micriscopy; BAM, biocompatible anchor for membrane; PEG, poly ethylene glycol; CLSM, confocal laser scanning microscopy;

1. Introduction

The mechanical features of cells are unique indicators of their states and constantly change in accordance with cellular events. During optic-cup morphogenesis, alterations in the level of stiffness of the retinal epithelium are important for the self-formation of neural retina tissue (Eiraku et al., 2011). Malignant cancer cells exhibit less stiffness than normal cells (Cross et al., 2007). Furthermore, the mechanical features of mesenchymal stem cells are attributed to their diverse characteristics and states (Kihara et al., 2011; Maloney et al., 2010; Sugitate et al., 2009; Titushkin and Cho, 2007). These mechanical changes in cells are widely mediated by actin cytoskeleton. Thus, by analyzing the mechanical properties of cells, it is possible to know and evaluate the characteristics of the complicated actin networks on the surface of cells. For example, studies analyzing the physical response of actin filaments networks (Chaudhuri et al., 2007), detecting the cell contraction force depending on cell substrate (Mitrossilis et al., 2009), and examining the penetration efficiency of fine nanoneedle through cell surface membrane (Kagiwada et al., 2010) have shown that the actin cytoskeleton can be potentially characterized by analyzing the mechanical properties of cells.

Actin cytoskeleton also controls the dynamic shape of cells during various morphological events. Thus analyzing the mechanical changes with the events helps elucidate the dynamical roles of actin cytoskeleton. During cell division, changes in the organization and dynamics of actin cytoskeleton cause retraction of the cell margin, cell rounding, and formation of the cleavage furrow (Cramer and Mitchison, 1997; Hickson et al., 2006; Kunda et al., 2008). The stiffness of the cleavage furrow region of cells in cytokinesis drastically increases as compared to that of the top region of cells in metaphase (Matzke et al., 2001). The cleavage furrow contains an actomyosin contractile ring, which controls the changes in stiffness of the region. Apart from this, cortical stiffness of metaphase rounded cells was greater than that of interphase adherent cells of *Drosophila* embryonic S2R+ cells (Kunda et al., 2008). Cortical rigidity and cell rounding at the onset of

mitosis are highly regulated by the ERM family of actin-binding proteins (ezrin, radixin, and moesin) (Kunda et al., 2008). ERM proteins crosslink the plasma membrane to the underlying actin-rich cortex by phosphorylated activation (Bretscher et al., 2002). Thus, activation of the ERM proteins is a key factor in cell rounding and formation of the rigid actin cortex during mitosis (Thery and Bornens, 2008).

Passive cell rounding, which is marked by a morphological change, can be induced by trypsin treatment. The surface morphology of trypsinized cell exhibits blebs, spherical protuberances, and microvillous projections (Harrison and Allen, 1979; Kinn and Allen, 1981). These surface morphological changes are similar to that during cell mitosis (Porter et al., 1973). Yamane et al. reported that detachment of HEK293T cells from the substrate by trypsinization and inhibition of reattachment induces phosphorylation of ERM proteins (Yamane et al., 2011). Thus, suspending the trypsinized round cells might induce the formation of a rigid actin cortex, similar to that observed during mitosis. Furthermore, suspended forms of adherent cells are found not only in artificial trypsinized condition but also in natural blood, e.g., metastatic cancerous cells and stem/progenitor cells (Hristov and Weber, 2004; Pantel et al., 2008; Stappenbeck and Miyoshi, 2009). Thus, the mechanical characterization of the actin cortex of the round-shaped cells helps elucidate the regulatory mechanisms underlying the dynamic morphological changes by the actin cytoskeleton.

Previously, we measured the stiffness of leukocytes and trypsinized cells by using atomic force microscopy (AFM) and a biocompatible anchor for membrane (BAM) substrate for anchoring the suspended cells (Kagiwada et al., 2010; Shimizu et al., 2012). In this study, we determined the cortical stiffness of the trypsinized round cells anchored by BAM substrate and compared it with that of mitotic round cells. To identify and examine the mitotic cells, Fucci system was employed. This system contains 2 fusion proteins, namely, the monomeric Kusabira Orange fused to human Cdt1 (mKO2-hCdt1) and the monomeric Azami Green fused to human geminin (mAG-hGeminin)

for visualizing the cell cycle phase (Sakaue-Sawano et al., 2008). Fucci system shows the cell cycle by phase-dependent color variation in fluorescence. Cells at the G_1/G_0 phase display red fluorescent nuclei, whereas those at the S/G_2 phase show green fluorescent nuclei. Mitotic cells with diminished nuclear membrane show green fluorescence of the entire cell, allowing the measurement of cortical stiffness of round cells by AFM. The mitotic and trypsinized round cells both showed actin-rich cortical regions on the cell surface. Although the cortical actin regions observed using confocal laser scanning microscopy (CLSM) were almost the same irrespective of the cell state, the cortical rigidity of trypsinized round cells showed greater stiffness as than that of mitotic round cells. Thus, the cortical rigidity of round cells varies according to the cell state, and analyzing the cell cortex rigidity is useful for characterizing the actin network on the cell surface.

2. Materials and Methods

2.1. Materials

A quadratic pyramidal AFM probe (SN-AF01-S-NT; spring constant: 0.02 N/m) was purchased from SII NanoTechnology Inc. (Chiba, Japan). Hela.S-Fucci (RCB2812) and NMuMG-Fucci (RCB2813) cells (Sakaue-Sawano et al., 2008) were obtained from RIKEN BioResource Center (Saitama, Japan) by permission of Dr. Atsushi Miyawaki (Riken, Japan). Cell culture medium was purchased from Sigma-Aldrich (St. Louis, MO). Fetal bovine serum (FBS) was purchased from JRH Biosciences (Lenexa, KS). Antibiotics were purchased from Life Technologies Japan Ltd. (Tokyo, Japan). BAM (SUNBRIGHT OE-020CS) was purchased from NOF CORPORATION (Tokyo, Japan). Other reagents were obtained from Sigma-Aldrich, Wako Pure Chemical Industries Ltd. (Osaka, Japan), or Life Technologies Japan Ltd. (Tokyo, Japan).

2.2. Preparation of BAM-coated dishes

BAM contains a membrane anchoring oleyl group, a hydrophilic poly ethylene glycol (PEG) domain, and an NHS-reactive ester group (Kato et al., 2003). The BAM-coated dishes were prepared as described previously (Shimizu et al., 2012). Briefly, polystyrene tissue culture dishes were coated with 5% BSA in PBS for 1 h. After washing with PBS, the surfaces were treated with 1 mM BAM in PBS for 30 min. Then, the BAM-coated dishes were washed and dried.

2.3. Cell cultures

Hela.S-Fucci and NMuMG-Fucci cells were maintained in DMEM containing 10% FBS and antibiotics (100 units/mL penicillin G and 100 μg/mL streptomycin sulfate). The culture medium was replaced three times a week. Cells were detached from the culture dish by treatment with 0.25% trypsin-0.02% EDTA in PBS and then plated on the BAM-coated dish for 3 h in culture medium. The cells attached to the BAM surface were manipulated by AFM (Fig. 1). Actin-depolymerization of the cells was induced by treatment with 2 μM cytochalasin D for 2 h.

2.4. AFM measurements

Hela.S-fucci and NMuMG-Fucci cells adhered to the tissue culture dishes or attached to the BAM-coated dishes in the medium were manipulated by AFM (Nanowizard I, JPK Instruments AG, Berlin, Germany) at room temperature. The AFM was combined with fluorescence microscope (IX71; Olympus, Tokyo, Japan) so that cell cycle phases could be determined by observing the Fucci fluorescence (Fig. 2). The probe indented the top of the cells up to 1 nN at 5 μm/s. The Young's modulus of the cell calculated in accordance with the Hertz model (Hertz, 1881). Unless otherwise indicated, the force-distance curve at the region up to approximately 300 nm of the cell surface indentation was fitted by JPK data processing software (JPK instruments AG) as follows:

$$F = \frac{E}{1-\nu^2}\frac{\tan\alpha}{\sqrt{2}}\delta^2,$$

where F = force, δ = depth of indentation, α = half angle to face of pyramidal probe (20 degree), ν =

Poisson's ratio (0.5), and E = Young's modulus (Fig. 1C).

All experiments performed using more than 20 cells, and each cell was examined at 25 points on the top of the cell. The median value adopted for the Young's modulus of each cell (Kihara et al., 2011).

2.5. F-actin imaging

The cells were fixed with 4% paraformaldehyde, permeabilized with 0.5% Triton X-100, and then stained with rhodamine-phalloidin for actin filaments. Specimens were observed by CLSM (FV-1000; Olympus) equipped with x60 oil immersion lens (NA = 1.42) in 0.5 μm serial sections. Superimposition of the serial images processed with ImageJ software (NIH, Bethesda, MD).

3. Results

3.1. Cortical actin imaging of Hela.S-Fucci and NMuMG-Fucci cells

One of the typical morphological characteristics of adherent mitotic cells is its spherical shape, yet it is difficult to discriminate mitotic round cells from other cells in various phases, including dead round-shaped cells. Therefore, this study used the Fucci system (Sakaue-Sawano et al., 2008) to determine the mitotic phase of adherent cells. Most of these cells showed clear green/red fluorescent nuclei; however, some round cells showed green fluorescence in the entire cell body (Fig. 2). Thus, we identified that cells with round shape and green fluoresce in whole cell body are in mitotic phase (Fig. 2).

Trypsinized detached cells were fixed on the BAM substrate (Fig. 1). The detached cells spontaneously attached to the BAM substrate and maintained a round shape (Fig. 1B). The attached cells anchored tightly and were not dislodged from the surface by swinging, which enabled AFM manipulation of the live round cells.

The mitotic and trypsinized round cells show activation of the ERM proteins (Kunda et al.,

2008; Yamane et al., 2011). These round cells may have developed cortical actin. To compare the cortical actin structure, F-actin of the mitotic and trypsinized round cells was stained. The adherent Hela.S-Fucci cells did not show any actin stress fibers but had many short microvillus protrusions on their surface (Fig. 3). The mitotic Hela.S-Fucci cells showed many long microvilli structures on their cell surface and F-actin-rich regions in the cortex (Fig. 3). The trypsinized round Hela.S-Fucci cells showed short microvilli structures on their surface and clear cortical actin filaments (Fig. 3). In NMuMG-Fucci cells, interphase adherent cells showed many actin filaments structures, basal stress fibers, and dense protrusions on their surface (Fig. 3). The mitotic NMuMG-Fucci cells had long retraction fibers, some short microvilli structures, and cortical actin structure (Fig. 3). The trypsinized NMuMG-Fucci cells showed developed cortical actin and many small blebb-like structures on their surface (Fig. 3). Emergence of many long microvilli protrusions and long retraction fibers in mitotic Hela.S-Fucci and NMuMG-Fucci cells is in agreement with the mitotic cell image by electron microscopy (Porter et al., 1973). Moreover, surface structure of trypsinized round cells was similar to the reports about surface morphological changes by trypsinization (Harrison and Allen, 1979; Kolata, 1975). The F-actin structures in mitotic and trypsinized round cells tended to be similar, with both cells showing a clear cortical actin on the cell surface.

3.2. Young's modulus of mitotic and trypsinized round cells

This study evaluated the mechanical properties of the cortical region of cells. At interphase, the Young's modulus of adhered NMuMG-Fucci cells was higher than that of Hela.S-Fucci cells (Fig. 4). The average value of the logarithmic Young's modulus of these cells was 7.7 kPa (NMuMG-Fucci cells) and 1.5 kPa (Hela.S-Fucci cells). During mitosis, the average values of the logarithmic Young's modulus of these cells decreased to 0.40 kPa (NMuMG-Fucci cells) and 0.60 kPa (Hela.S-Fucci cells) (Fig. 4). In contrast, the average values of the logarithmic Young's modulus of these cells after trypsinization and attachment to the BAM surface were 1.8 kPa (NMuMG-Fucci

cells) and 1.9 kPa (Hela.S-Fucci cells) (Fig. 4). These round cells at either condition showed almost the same degree of stiffness in NMuMG-Fucci and Hela.S-Fucci cells. However, the cortical rigidity of trypsinized round cells was apparently greater than that of mitotic round cells. These Young's modulus values were higher than those of cytochalasin D-treated actin-depolymerized cells (Fig. 4). Therefore, these obtained mechanical properties during each condition reflect the mechanical characteristics of actin networks around the cell surface.

Although most studies have fitted the force-distance curve to the Hertz model at small indentation region from cell surface (around 300 nm here), the nanoindentation measurement by AFM can even detect the surface brush structure of cells (Iyer et al., 2009). However, the mitotic cells showed relatively long microvilli protrusions on their surface compared to trypsinized round cells (Fig. 3), which might have affected our results. To check this possibility, we calculated the apparent Young's modulus of each cell using the region at the indentation region of maximum 600 to 1000 pN of Force-distance curve. The result, which is shown in the supplementary Fig. S1 indicated that the trypsinized cells were indeed stiffer than mitotic cells. Thus, our experiments showed the stiffness of the cell cortex but not the surface protrusions, and most importantly, the rigidity of cortical actin in the round-shaped cells changed during different cell conditions.

4. Discussion

This study showed that the cortical rigidities of round-shaped cells in mitosis and in trypsinized-detached state are different. In the latter state, the cell cortex was stiffer than that of mitotic round cells (Fig. 4). The difference in the mechanical properties of the cell cortex is inconsistent with the results obtained by CLSM imaging of F-actin (Fig. 3). The mechanical properties of the actin cytoskeleton showed a possible qualitative actin construction of the cell surface, which is different from their morphological structures. Thus, the elucidation of these

qualitative features of actin cytoskeleton around the cell surface will help determine the regulatory mechanism underlying cell dynamics and morphology.

The process of cell rounding in mitotic *Drosophila* S2R+ cells is mainly controlled by ERM and moesin proteins (Kunda et al., 2008). At the onset of mitosis of S2R+ cells, activated moesin helps in the conversion of protrusive lamellipodial actin structures, which are predominantly present during interphase, into a uniform cortex in which the actin filaments lie parallel to the plane of the plasma membrane; this uniform cortex is the characteristic feature of mitotic cells. In particular, ERM proteins, rather than myosin II, play a major role in cell rounding and cortical rigidity. Some studies have reported that stiffness of the cell cortex increases as they enter mitosis (Kunda et al., 2008; Matzke et al., 2001). However, in our study, the cortical rigidity of Hela.S-Fucci and NMuMG-Fucci cells in mitosis was lower than that of adherent interphase cells (Fig. 4). In case of NMuMG-Fucci cells, many actin fibers and dense surface protrusions in adherent interphase cells diminished in mitotic phase (Fig. 3), and thus the stiffness decline is small wonder. On the other hand, Hela.S-Fucci cells had many F-actin microvilli protrusions on their cell surface both in interphase and mitotic phase. Yet, it is unclear why the surface stiffness decreased in mitotic phase.

In contrast, cortical rigidity of trypsinized round cells was greater than that of mitotic cells (Fig. 4). Especially trypsinized Hela.S-Fucci cells were slightly stiffer than that of interphase cells (Fig. 4). CLSM analysis of F-actin structures showed that both mitotic and trypsinized round cells similarly induced the formation of actin cortex (Fig. 3). Thus, although the development and solidity of the cortical actin may appear the same in both mitotic and trypsinized cells, they generate different mechanical phenotype during mitosis and detachment.

There are several known differences between physical properties of mitotic and trypsinized cells. Stewart et al. reported that rounding pressure, generated by an osmotic pressure, of mitotic cells (including prometaphase and metaphase) is more than 3-fold higher than that of trypsinized

cells (Stewart et al., 2011). In addition, the surface area and volume of cells decrease as they round and enter metaphase due to depletion of surface membrane reservoir through preventing the secretion and recycling the membrane traffic (Boucrot and Kirchhausen, 2007, 2008). This finding indicates that cells probably control their internal osmotic pressure by changing their volume and surface area. On the other hand, the cell surface of trypsinized cells is the same as untreated cells (Boucrot and Kirchhausen, 2007). Therefore unlike mitotic cells, the endosomal recycling and surface membrane reservoir, which is associated with membrane tension (Raucher and Sheetz, 1999), would be normal in trypsinized cells.

Since the surface tension is balanced with osmotic pressure, surface membrane reservoir, cell radius, and actomyosin cortex, we assumed that trypsinized cell, with normal membrane reservoir, cell radius, and weak rounding osmotic pressure, highly maintains its shape via actomyosin cortex which is an important factor for surface tension in trypsinized round cell. Moreover, Maloney et al. reported that the surface bleb formation of trypsinized floating cell decreases with time and that the rigidity of trypsinized cell increases within 60 min (Maloney et al., 2010). Our AFM measurements for trypsinized cells were conducted after 3h incubation on BAM surface during which the cells' actomyosin cortex could have become fully developed. On the other hand, the mitotic round cells with high osmotic pressure, relatively small cell radius, and low surface membrane reservoir, may require to minimize the maintaining round force. Moreover, the combined period of prometaphase and metaphase during mitosis is around 60 min in many cases. This period may be relatively short for the cell to fully develop actomyosin cortex structure. The widely varied Young's modulus in mitoic cells probably indicates the affect of the alterations of osmotic pressure and actin cortex (Fig. 4). In sum, the strength of the actomyosin cortex would be higher in trypsinized round cells compared to mitotic (prometaphase and metaphase) cells.

Other assumptions for the difference between Young's modulus of round trypsinized cell and mitotic cell are conceived as follows. One is the difference of cell shape. The morphology of

trypsinized detached cell is almost spherical, however, the height-to-width ratio in metaphase cell is 0.86 which indicates an oval shape (Stewart et al., Nature, 469, 226-230, 2011). The bottom-to-side region of the oval mitotic cell contains many retraction fibers which anchor to actin cortex (Thery et al., 2005). Thus, the cortical actin density or strength of the top region of oval-shaped mitotic cell may be small compared to both the bottom-to-side region of the oval shape and to the trypsin treated cell with complete spherical shape. The other is that trypsinized round cell can maintain some F-actin structures on the cell surface. The mechanism of redistribution of actin filaments structures to a relatively uniform cortex in trypsinized round cells remains unclear. For this reason, trypsinized round Hela.S-Fucci cells with cortical actin and some surface F-actin structures might show more stiffness than interphase cells (Fig. 4). However, further investigation of the regulatory mechanism underlying cell rounding by ERM proteins is required.

Meanwhile, no defined differences were observed in phalloidin labelled F-actin cortices of round mitotic and trypsinized cells (Fig. 3). The CLSM imaging of F-actin makes a significant contribution to determination of their localization but it can hardly provide information about the maturation or strength of F-actin structures. The AFM nanoindentation method, however, tackles this issue and measures the mentioned parameters.

In this study, we used Fucci system expressing cells. The Fucci system is a fluorescent indicator for the cell cycle (Sakaue-Sawano et al., 2008). Thus, it is possible to compare the surface stiffness of cells at the G_0/G_1 phase with that of cells at the S/G_2 phase. We randomly measured the surface stiffness of interphase cells, but we could not find cluster of each cell phase (Fig. 4). Hence, to examine the delicate difference between cell surface stiffness and cell cycle stages, especially G_1, S, and G_2 phases, high-precision tools and discriminatory methods for S- and G_2-phase cells are needed.

In summary, cortical rigidity of round cells varies according to the cell state, and the analysis of the mechanical properties of the cell cortex by AFM proves to be a useful method for

evaluating the complex actin cytoskeleton network of cell surface. In the future, to clarify and evaluate the actomyosin cortex of trypsinized cells, we will examine the effects of the osmotic pressure and shape on the cortical rigidity of trypsinized cells. Furthermore, we plan to investigate the mechanical role of actomyosin cortex in various cell types and states using some actin-perturbing agents and then evaluate the homology and discrepancy between fluorescence imaging and AFM measurements. We also intend to examine the mechanics and organization of actin cytoskeleton of spontaneously detached metastatic cancerous cells by using our suspended cell measuring method.

Acknowledgements

This work was supported by grants from Okinawa Prefecture, Japan (research project of industrialization of medical innovation and technology to J.M.) and Graduate School of Engineering Science, Osaka University, Japan (Multidisciplinary Research Laboratory System to T.K.).

References

Boucrot, E., Kirchhausen, T., 2007. Endosomal recycling controls plasma membrane area during mitosis. Proc Natl Acad Sci U S A 104, 7939-7944.

Boucrot, E., Kirchhausen, T., 2008. Mammalian cells change volume during mitosis. PLoS One 3, e1477.

Bretscher, A., Edwards, K., Fehon, R.G., 2002. ERM proteins and merlin: integrators at the cell cortex. Nat Rev Mol Cell Biol 3, 586-599.

Chaudhuri, O., Parekh, S.H., Fletcher, D.A., 2007. Reversible stress softening of actin networks. Nature 445, 295-298.

Cramer, L.P., Mitchison, T.J., 1997. Investigation of the mechanism of retraction of the cell margin and rearward flow of nodules during mitotic cell rounding. Mol Biol Cell 8, 109-119.

Cross, S.E., Jin, Y.S., Rao, J., Gimzewski, J.K., 2007. Nanomechanical analysis of cells from cancer patients. Nat Nanotechnol 2, 780-783.

Eiraku, M., Takata, N., Ishibashi, H., Kawada, M., Sakakura, E., Okuda, S., Sekiguchi, K., Adachi, T., Sasai, Y., 2011. Self-organizing optic-cup morphogenesis in three-dimensional culture. Nature 472, 51-56.

Harrison, C.J., Allen, T.D., 1979. Cell surface morphology after trypsinisation depends on initial cell shape. Differentiation 15, 61-66.

Hertz, H., 1881. Über die berührung fester elastischer Körper. J. reine und angewandte Mathematik 92, 156-171.

Hickson, G.R., Echard, A., O'Farrell, P.H., 2006. Rho-kinase controls cell shape changes during cytokinesis. Curr Biol 16, 359-370.

Hristov, M., Weber, C., 2004. Endothelial progenitor cells: characterization, pathophysiology, and possible clinical relevance. J Cell Mol Med 8, 498-508.

Iyer, S., Gaikwad, R.M., Subba-Rao, V., Woodworth, C.D., Sokolov, I., 2009. Atomic force microscopy detects differences in the surface brush of normal and cancerous cells. Nat Nanotechnol 4, 389-393.

Kagiwada, H., Nakamura, C., Kihara, T., Kamiishi, H., Kawano, K., Nakamura, N., Miyake, J., 2010. The mechanical properties of a cell, as determined by its actin cytoskeleton, are important for nanoneedle insertion into a living cell. Cytoskeleton (Hoboken) 67, 496-503.

Kato, K., Umezawa, K., Funeriu, D.P., Miyake, M., Miyake, J., Nagamune, T., 2003. Immobilized culture of nonadherent cells on an oleyl poly(ethylene glycol) ether-modified surface. Biotechniques 35, 1014-1018, 1020-1011.

Kihara, T., Haghparast, S.M., Shimizu, Y., Yuba, S., Miyake, J., 2011. Physical properties of mesenchymal stem cells are coordinated by the perinuclear actin cap. Biochem Biophys Res Commun 409, 1-6.

Kinn, S.R., Allen, T.D., 1981. Conversion of blebs to microvilli: cell surface reorganisation after trypsin. Differentiation 20, 168-173.

Kolata, G.B., 1975. Microvilli: a major difference between normal and cancer cells? Science 188, 819-820.

Kunda, P., Pelling, A.E., Liu, T., Baum, B., 2008. Moesin controls cortical rigidity, cell rounding, and spindle morphogenesis during mitosis. Curr Biol 18, 91-101.

Maloney, J.M., Nikova, D., Lautenschlager, F., Clarke, E., Langer, R., Guck, J., Van Vliet, K.J., 2010. Mesenchymal stem cell mechanics from the attached to the suspended state. Biophys J 99, 2479-2487.

Matzke, R., Jacobson, K., Radmacher, M., 2001. Direct, high-resolution measurement of furrow stiffening during division of adherent cells. Nat Cell Biol 3, 607-610.

Mitrossilis, D., Fouchard, J., Guiroy, A., Desprat, N., Rodriguez, N., Fabry, B., Asnacios, A., 2009. Single-cell response to stiffness exhibits muscle-like behavior. Proc Natl Acad Sci U S A 106, 18243-18248.

Pantel, K., Brakenhoff, R.H., Brandt, B., 2008. Detection, clinical relevance and specific biological properties of disseminating tumour cells. Nat Rev Cancer 8, 329-340.

Porter, K., Prescott, D., Frye, J., 1973. Changes in surface morphology of Chinese hamster ovary cells during the cell cycle. J Cell Biol 57, 815-836.

Raucher, D., Sheetz, M.P., 1999. Membrane expansion increases endocytosis rate during mitosis. J Cell Biol 144, 497-506.

Sakaue-Sawano, A., Kurokawa, H., Morimura, T., Hanyu, A., Hama, H., Osawa, H., Kashiwagi, S., Fukami, K., Miyata, T., Miyoshi, H., Imamura, T., Ogawa, M., Masai, H., Miyawaki, A., 2008. Visualizing spatiotemporal dynamics of multicellular cell-cycle progression. Cell 132, 487-498.

Shimizu, Y., Kihara, T., Haghparast, S.M.A., Yuba, S., Miyake, J., 2012. Simple display system of mechanical properties of cells and their dispersion. PLoS ONE, in press. doi: 10.1371/journal.pone.0034305.

Stappenbeck, T.S., Miyoshi, H., 2009. The role of stromal stem cells in tissue regeneration and wound repair. Science 324, 1666-1669.

Stewart, M.P., Helenius, J., Toyoda, Y., Ramanathan, S.P., Muller, D.J., Hyman, A.A., 2011. Hydrostatic pressure and the actomyosin cortex drive mitotic cell rounding. Nature 469, 226-230.

Sugitate, T., Kihara, T., Liu, X.-Y., Miyake, J., 2009. Mechanical role of the nucleus in a cell in terms of elastic modulus. Current Applied Physics 9, e291-e293.

Thery, M., Bornens, M., 2008. Get round and stiff for mitosis. Hfsp J 2, 65-71.

Thery, M., Racine, V., Pepin, A., Piel, M., Chen, Y., Sibarita, J.B., Bornens, M., 2005. The extracellular matrix guides the orientation of the cell division axis. Nat Cell Biol 7, 947-953.

Titushkin, I., Cho, M., 2007. Modulation of cellular mechanics during osteogenic differentiation of human mesenchymal stem cells. Biophys J 93, 3693-3702.

Yamane, J., Ohnishi, H., Sasaki, H., Narimatsu, H., Ohgushi, H., Tachibana, K., 2011. Formation of microvilli and phosphorylation of ERM family proteins by CD43, a potent inhibitor for cell adhesion: cell detachment is a potential cue for ERM phosphorylation and organization of cell morphology. Cell Adh Migr 5, 119-132.

Figure legends

Fig. 1 AFM manipulation. (A) A diagram of the BAM-coated substrate. BAM molecules are fixed on the BSA-coated substrate. The surface oleyl group enters the plasma membrane of the cell, thereby anchoring the cell onto the BAM substrate. (B) Phase-contrast micrograph of Hela.S-Fucci cells on the BAM substrate. The trypsinized detached cells were anchored to the substrate, which allowed them to maintain their round shape. The object on the left is the AFM cantilever. (C) Typical force-distance curve obtained from the AFM indentation experiments with adherent interphase Hela.S-Fucci cells. The black points show experimental force curve lines, and the gray line shows the Hertz model fitting line. The force-distance curve at the region approximately 300 nm of cell surface indentation was fitted to the Hertz model.

Fig. 2 Fluorescence images of Fucci system. The Hela.S-Fucci and NMuMG-Fucci cells were cultured in normal culture dishes. The phase-contrast image (PH), green fluorescence image (mAG-hGeminin), red fluorescence image (mKO2-hCdt1), and merged image (Merge) are displayed. Green fluorescent nuclei and red fluorescent nuclei are shown in the spreading cells. Mitotic cells are round and emit green fluorescence (arrowheads).

Fig. 3 CLSM images of F-actin. F-actin structures in Hela.S-Fucci and NMuMG-Fucci cells during interphase, mitosis, and trypsinized round states were observed by CLSM. The superposition images of cell top, middle part, and whole cell are shown. Thickness of each superposition (a: top, b: middle, or c: whole) is shown in each image. All the indicated cells originally expressed mAG-hGeminin ($S/G_2/M$ phase), and F-actin was labeled with rhodamine-phalloidin. The mitotic cell is larger than that of trypsinized round cell. Middle part images clearly indicate the cortical actin structure of the cells. Bar = 20 μm.

Fig. 4　Young's modulus of Hela.S-Fucci and NMuMG-Fucci cells under various conditions. Young's moduli of the cell surface during interphase, mitotic phase, trypsinized round state, and cytochalasin D treatment (CD) are shown. The scale of Young's modulus is logarithm. Each condition shows the Young's modulus of 20 independent cells and each cell was measured 25 times on the cell top.

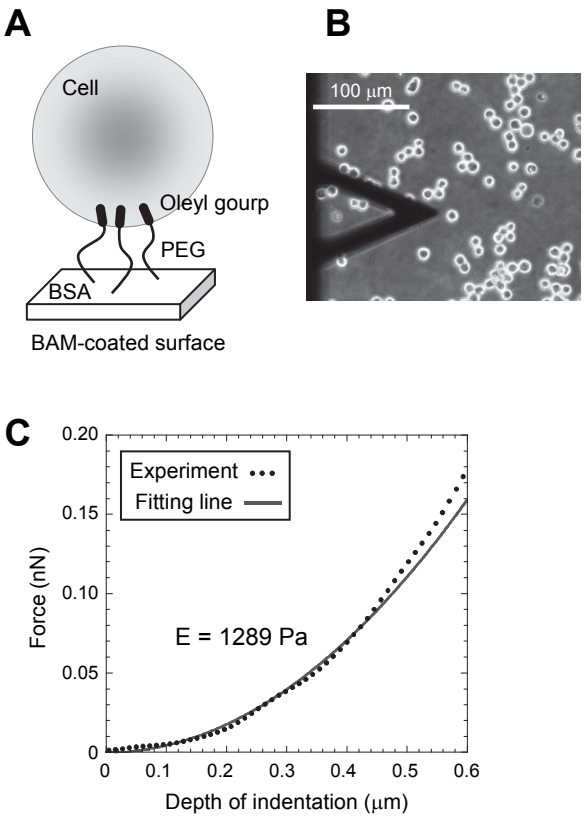

Fig. 1 Shimizu et al.

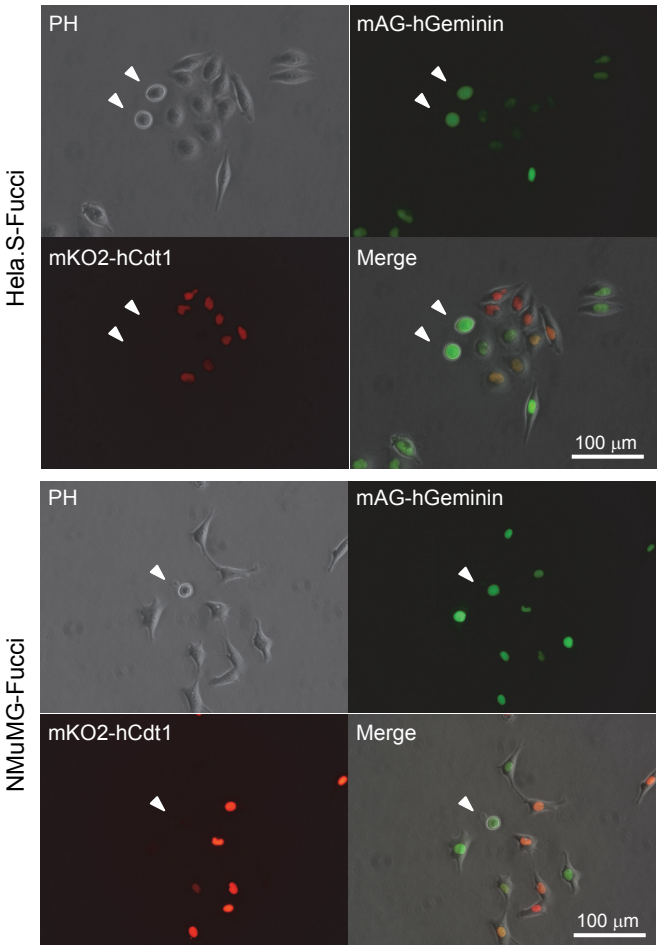

Fig. 2 Shimizu et al.

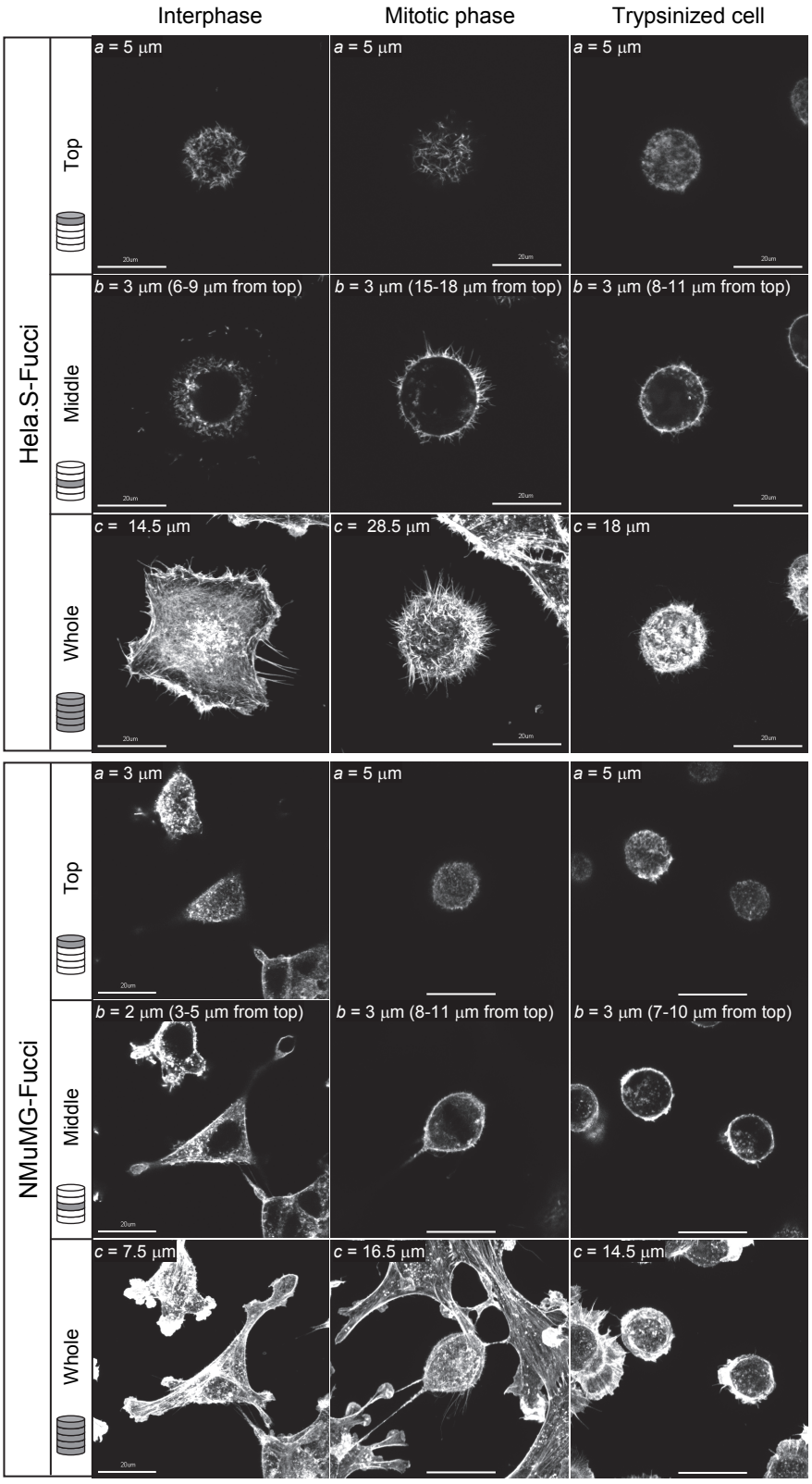

Fig. 3 Shimizu et al.

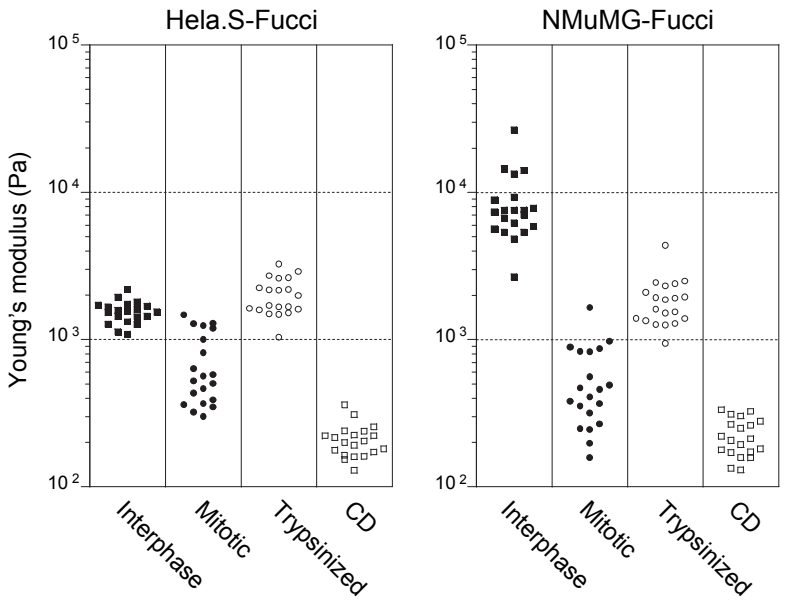

Fig. 4 Shimizu et al.

Supplementary Figure

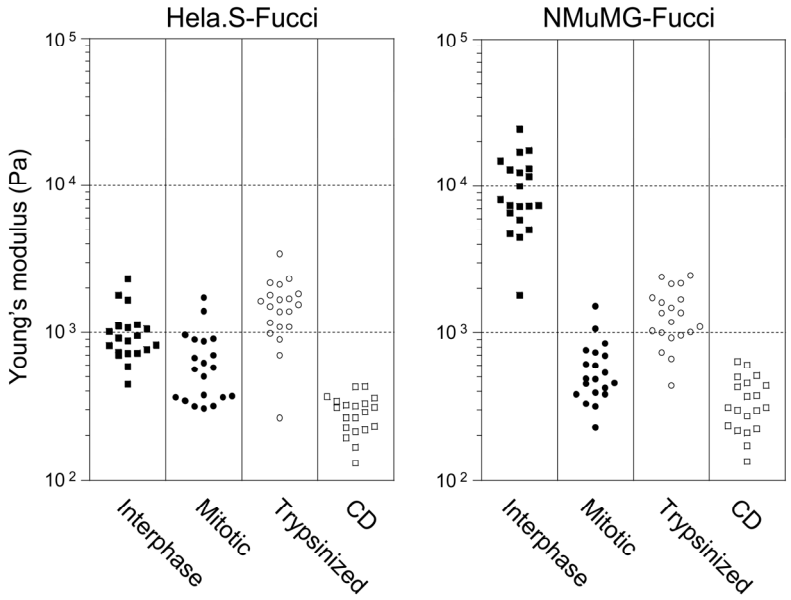

Supplementary Fig. S1. Apparent Young's modulus of Hela.S-Fucci and NMuMG-Fucci cells using the region at the indentation region of maximum 600 to 1000 pN of Force-distance curve. The apparent Young's moduli of the cell surface during interphase, mitotic phase, trypsinized round state, and cytochalasin D treatment (CD) are shown. The scale of Young's modulus is logarithmic. Each condition shows the Young's modulus of 20 independent cells and each cell was measured 25 times on the cell top. The pattern that the trypsinized cells were stiffer than mitotic cells, was unalterable.